Genes & Diseases (2022) 9, 1401–1404

Available online at www.sciencedirect.com

ScienceDirect

journal homepage: http://ees.elsevier.com/gendis/default.asp

RAPID COMMUNICATION

HBV sL13H mutation impairs its surface antigen expression and ability to induce autophagy

To the Editor,

Autophagy, a conserved "self-eating" process for cellular homeostasis, plays a crucial role in the hepatitis B virus (HBV) life cycle, including viral assembly, envelopment, release, and degradation.[1] Autophagy can also be hijacked by HBV for its persistence and survival. However, the association between HBV mutations and autophagy remains unclear. Herein, we found that an HBV surface antigen (HBsAg) mutation involving sL13H substitution impaired HBsAg expression and caused its abnormal distribution *in vitro* and in a hydrodynamic injection (HI)-based mouse model for acute HBV infection. The sL13H mutation also decreased autophagosome formation and inhibited autophagic flux. Further mechanistic analysis revealed that sL13H suppresses HBV-induced autophagy initiation by inhibiting the eukaryotic translation initiation factor 2 alpha kinase 3 (EIF2AK3/PERK)—eukaryotic translation initiation factor 2 subunit alpha (EIF2S1/eIF2α)—autophagy related (ATG)5/12 axis. Therefore, our findings reveal a potential role for HBV mutations in manipulating host autophagic flux for virus persistence and pathogenesis in chronic hepatitis B.

HBsAg mutations affect virion assembly, stability, or infectivity associated with ground glass hepatocyte formation and hepatocellular carcinoma.[2] However, it remains unclear whether and how HBV mutations, such as the preS/S gene variants,[3] influence host autophagic flux. Previously, we identified the HBsAg sL13H mutation in samples from patients with chronic HBV infection.[3] Here, to investigate the impact of sL13H on HBsAg expression, mutant or wild type (WT) sequence was introduced into an HBV replication-competent plasmid that was then transfected into Huh7 or HepG2 cells. Western blot analysis showed that the total amount of HBsAg, including large, middle, and small HBsAg, significantly decreased for the sL13H mutant compared with that for the WT (Fig. 1A, B). Consistently, the levels of secreted and intracellular HBsAg also decreased, as determined using measured by enzyme-linked immunosorbent assay (Fig. 1C, S1A). Similar results were obtained in Huh7 cells (Fig. S1B), when sL13H was introduced into the WT HBsAg sequence in the backbone vector pXF3H as described previously.[4] We further assessed the impact of sL13H on subcellular HBsAg distribution. The intracellular HBsAg level significantly decreased in HBV-sL13H-transfected Huh7 cells, as determined using anti-HBs staining (Fig. 1D, S1C). WT HBsAg was evenly distributed throughout the cytoplasm of the transfected cells, whereas HBsAg with sL13H exhibited dot-like accumulation in the perinuclear endoplasmic reticulum (ER), as determined using immunofluorescence staining for the ER marker protein calnexin (Fig. S1D). Therefore, sL13H impairs HBsAg production and causes its abnormal distribution.

The impact of sL13H on HBsAg expression was further investigated in an HI-based mouse model for acute HBV infection. Following HI of the HBV construct pHBV1.3 into C57BL/6 mice, serum HBsAg levels were monitored from 1 to 21 days post injection (dpi) (Fig. S2A). In the WT group, HBsAg levels peaked at 4 dpi, then declined and were undetectable at 10 dpi (Fig. S2B). However, in sera collected from the sL13H group, HBsAg was undetectable throughout the monitoring period (Fig. S2B). HBsAg staining was stronger in the liver tissues of the WT group at 4 and 7 dpi than in the sL13H group; few hepatocytes stained positive in the sL13H group at 7 dpi (Fig. S2C). These results further verified that sL13H impairs HBsAg expression in the mouse model.

To assess whether sL13H affects host autophagy, the expression and localization of LC3, an autophagy marker protein, were analyzed using immunofluorescence staining. Compared with that in cells expressing WT HBsAg, the number of LC3 puncta decreased in Huh7 cells expressing

Peer review under responsibility of Chongqing Medical University.

https://doi.org/10.1016/j.gendis.2022.01.004

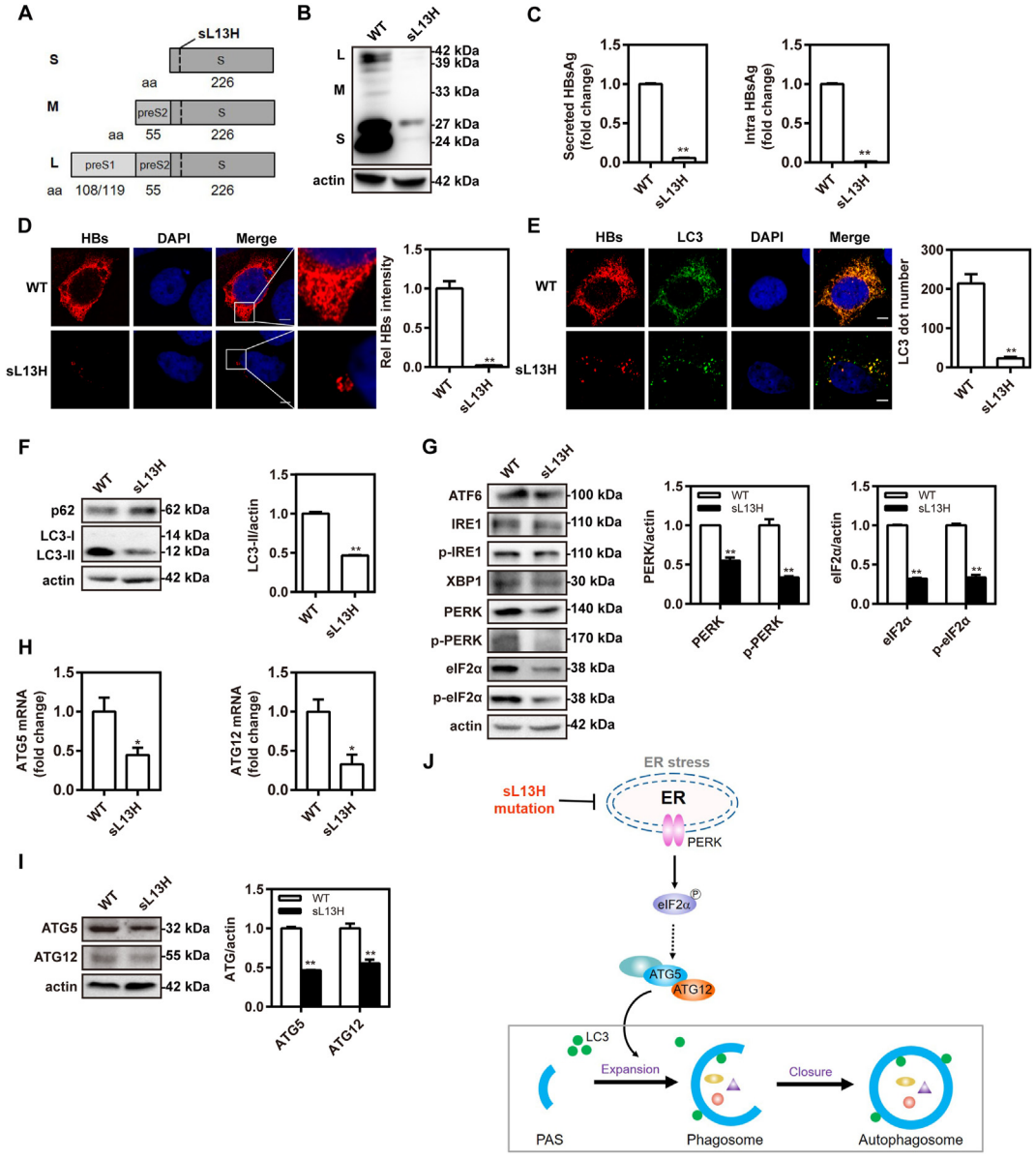

Figure 1 HBV sL13H impairs HBsAg expression and ability to induce autophagy by inhibiting the PERK-eIF2α-ATG5/12 axis. **(A)** Schematic representation of the position of the sL13H mutation in the small (S), middle (M), and large (L) surface protein. **(B–I)** Huh7 cells were transfected with plasmid pHBV1.3-WT (WT) or pHBV1.3-sL13H (sL13H). (B) At 72 h post-transfection, the expression of L-, M-, and S-HBsAg was detected by western blotting. β-actin served as a loading control. (C) Secreted and intracellular HBsAg were detected using ELISA. (D) At 48 h post-transfection, cells were fixed and stained for HBsAg staining. Their nuclei were stained with DAPI. Finally, the cells were imaged by confocal microscopy. Scale bar: 5 μm. The fluorescence intensity of HBs were analyzed using ImageJ software. (E) At 48 h post-transfection, cells were fixed and incubated with horse anti-HBs and rabbit anti-LC3 antibodies, followed by staining with Alexa Fluor 488-conjugated anti-rabbit IgG and Alexa Fluor 594-conjugated anti-horse IgG antibodies. The expression of HBsAg and LC3 was observed by confocal microscopy. Scale bars, 5 μm. The numbers of LC3 dots were calculated using ImageJ software. (F) At 48 h post-transfection, intracellular p62 and LC3 proteins were detected via western blotting. The relative intensities of both LC3II and β-actin were calculated and the result was represented as the ratio of LC3II to β-actin. (G) Autophagy-related proteins, including ATF6, IRE-1, phosphorylated IRE1 (p-IRE1), XBP1, PERK, phosphorylated PERK (p-PERK), eIF2α, and phosphorylated eIF2α (p-eIF2α), were detected by western blotting. The gray values of target proteins (PERK, p-PERK, eIF2α, and p-eIF2α) and β-actin were analyzed and the results were calculated and represented as the ratio of these target proteins to β-actin. (H) At 72 h post-transfection, intracellular total RNA was extracted, followed by detecting ATG5 and ATG12 mRNA levels using real-time RT-PCR. (I) ATG5 and ATG12 protein levels were detected by western blotting. The relative intensities of ATG5, ATG12, and β-actin were calculated and the result was represented as the ratio of ATG5 or ATG12 to β-actin. * $P < 0.05$; ** $P < 0.01$; ns, not significant. (J) A proposed model depicting the interference of HBV-induced autophagy via inhibiting PERK-eIF2α-ATG5/12 axis by HBsAg mutation with sL13H substitution.

HBsAg with sL13H (Fig. 1E). The LC3 levels decreased in sL13H-transfected Huh7 cells, whereas those of the autophagic receptor p62 correspondingly increased (Fig. 1F), indicating that sL13H interferes with HBV-induced autophagy initiation. We further observed that lower levels of green fluorescent protein (GFP)-tagged-LC3 and mCherry-LC3 expression for sL13H than for the WT (Fig. S3A), confirming that sL13H impairs the HBV-induced autophagy initiation. To assess the effect of sL13H in the context of blocking autophagic degradation, Huh7 cells were treated with the lysosome inhibitor glucosamine (GlcN) after HBV transfection. Consistently, sL13H had no promoting effect on HBsAg secretion in cells with GlcN treatment (Fig. S3B), thus providing further evidence on the inhibitory role of sL13H in HBV-induced autophagy initiation.

HBsAg accumulation can cause ER stress and induce the unfolded protein response (UPR) via the activating transcription factor 6 (ATF6), inositol-requiring protein-1 (IRE1), or PERK signaling pathways, which may contribute to autophagy induction.[1] Therefore, we next sought to identify the protein kinase signaling pathway involved in inhibiting autophagy induction in the presence of sL13H. Real-time reverse transcription-polymerase chain reaction showed that *ATF6* or *IRE1* mRNA levels did not significantly change in the presence of sL13H (Fig. S4A, B), whereas those of *PERK* mRNA significantly decreased (Fig. S4C). Correspondingly, the levels of total and phosphorylated PERK decreased (Fig. 1G). Additionally, total and phosphorylated eIF2α (downstream molecule of PERK signaling) levels also significantly decreased. Therefore, the HBV sL13H mutation inhibits activation of the PERK—eIF2α signaling axis.

Following PERK—eIF2α signaling inhibition, its downstream molecules may be involved as autophagy-associated proteins to induce autophagy.[1] Therefore, we subsequently analyzed the transcript levels of several critical genes associated with autophagy induction, including *JNK*, *BECN1*, *ATG5*, *ATG7*, and *ATG12*. Interestingly, *ATG5* and *ATG12* mRNA levels significantly decreased in HBV-sL13H-transfected cells (Fig. 1H), whereas those of *JNK*, *BECN1*, and *ATG7* mRNA did not significantly changed (Fig. S4D—F). Moreover, ATG5 and ATG12 protein levels also decreased (Fig. 1I). Collectively, these results suggest that HBV sL13H interferes with virus-induced autophagy by inhibiting the PERK—eIF2α—ATG5/12 axis (Fig. 1J).

Various mutation types in different HBV genome regions (including the preS1, preS2, core, and X regions) are reported to cause ER stress and result in distinct liver disease outcomes, in particular.[2] Different UPR sensors are likely to be involved in the role of HBV variants in ER stress.[1] For instance, Lee et al reported that an occult infection-related surface antigen variant can significantly activate all three UPR sensors.[5] Therefore, different HBV variants may differ in their capacity to induce ER stress, resulting in variable clinical outcomes.[2] In the present study, the HBV sL13H mutation inhibited activation of the PERK—eIF2α axis, suggesting that induction of ER stress. UPR induction is associated with autophagy induction[1]; whereas the degree of impact HBsAg mutations have on autophagy is currently unknown. We found that the sL13H substitution interferes with HBV induction of host autophagy by inhibiting PERK—eIF2α—ATG5/12 axis, which functions to block phagophore elongation and autophagosome maturation.[1] HBV sL13H can potentially manipulate autophagy for virus persistence and pathogenesis in chronic hepatitis B. Further studies are warranted to characterize discrete outcomes associated with different HBV variants.

Author contributions

ML, CW, and YL designed the research. JX, CW, and YL wrote and revised the paper. JX, LC, ZZ, YD, and YL performed the experiments. All authors contributed to the article and approved the submitted version.

Conflict of interests

The authors declare no conflicts of interests.

Funding

This work was supported by grants from the National Natural Science Foundation of China (No. 82002131, 31770180), the Natural Science Foundation Project of CQ CSTC (No. cstc2020jcyj-msxmX0081), and Open project of State Key Laboratory of Virology (No. 2020IOV006).

Appendix A. Supplementary data

Supplementary data to this article can be found online at https://doi.org/10.1016/j.gendis.2022.01.004.

References

1. Lin Y, Zhao Z, Huang A, Lu M. Interplay between cellular autophagy and hepatitis B virus replication: a systematic review. *Cells*. 2020;9(9):2101.
2. Choi YM, Lee SY, Kim BJ. Naturally occurring hepatitis B virus mutations leading to endoplasmic reticulum stress and their contribution to the progression of hepatocellular carcinoma. *Int J Mol Sci*. 2019;20(3):597.
3. Cao L, Wu C, Shi H, et al. Coexistence of hepatitis B virus quasispecies enhances viral replication and the ability to induce host antibody and cellular immune responses. *J Virol*. 2014;88(15):8656—8666.
4. Wu C, Deng W, Deng L, et al. Amino acid substitutions at positions 122 and 145 of hepatitis B virus surface antigen (HBsAg) determine the antigenicity and immunogenicity of HBsAg and influence in vivo HBsAg clearance. *J Virol*. 2012;86(8):4658—4669.
5. Lee IK, Lee SA, Kim H, Won YS, Kim BJ. Induction of endoplasmic reticulum-derived oxidative stress by an occult infection related S surface antigen variant. *World J Gastroenterol*. 2015;21(22):6872—6883.

Jianbo Xia[a], Liang Cao[b], Zhenyu Zhao[c], Yingying Deng[c], Mengji Lu[d], Chunchen Wu[a,**], Yong Lin[c,*]

[a] *Department of Laboratory Medicine, Maternal and Child Health Hospital of Hubei Province, Tongji Medical College,*

Huazhong University of Science and Technology, Wuhan, Hubei 430070, PR China
[b] *Department of Microbiology and Immunology, Feinberg School of Medicine, Northwestern University, Chicago, IL 60208, USA*
[c] *Key Laboratory of Molecular Biology of Infectious Diseases (Chinese Ministry of Education), Chongqing Medical University, Chongqing 400016, PR China*
[d] *Institute of Virology, University Hospital Essen, University of Duisburg-Essen, 47048 Duisburg, Germany*

*Corresponding author. Key Laboratory of Molecular Biology of Infectious Diseases (Chinese Ministry of Education), Department of Infectious Diseases, The Second Affiliated Hospital, Institute for Viral Hepatitis, Chongqing Medical University, No.1 Yixueyuan Road, Yuzhong District, Chongqing 400016, PR China. Fax: +86 2368486780.

**Corresponding author. Department of Laboratory Medicine, Maternal and Child Health Hospital of Hubei Province, Tongji Medical College, Huazhong University of Science and Technology, No.745 Wuluo Road, Wuhan, Hubei 430070, PR China.
E-mail addresses: chunchen_wu@126.com (C. Wu), linyong@cqmu.edu.cn (Y. Lin)

3 November 2021
Available online 2 March 2022